Voyager 1/UVS Lyman α glow data from 1993 to 2003: Hydrogen distribution in the upwind outer heliosphere

Eric Quémerais, Jean-Loup Bertaux, and Rosine Lallement
Service d'Aéronomie du CNRS, Verrières le Buisson, France

Bill R. Sandel
Lunar and Planetary Laboratory, University of Arizona, Tucson, USA

Vlad Izmodenov
Institute for Problems in Mechanics, Moscow, Russia

Received 31 January 2003; revised 14 May 2003; accepted 29 May 2003; published XX Month 2003.

[1] We report the latest study of the UVS/Voyager 1 Lyman α data obtained between 1993 and 2003. These data show that the radial variation of the intensities measured close to the upwind direction has changed abruptly at the end of 1997 when the spacecraft was at a distance larger than 70 AU from the Sun. The coefficient α of the power law describing the intensity as a function of solar distance has changed from a value of −1.58 ± 0.02 between 1993 to 1997 to a value of −0.22 ± 0.07 after 1998. This change is not compatible with current stationary models of the hydrogen distribution whether they include the effects of the heliospheric interface or not. We discuss possible causes for this change including temporal variations of the hydrogen distribution near the heliopause. *INDEX TERMS:* 2124 Interplanetary Physics: Heliopause and solar wind termination; 2144 Interplanetary Physics: Interstellar gas; 2151 Interplanetary Physics: Neutral particles; 2162 Interplanetary Physics: Solar cycle variations (7536)

Citation: Quémerais, E., J.-L. Bertaux, R. Lallement, B. R. Sandel, and V. Izmodenov, Voyager 1/UVS Lyman α glow data from 1993 to 2003: Hydrogen distribution in the upwind outer heliosphere, *J. Geophys. Res.*, *108*(A10), 8029, doi:10.1029/2003JA009871, 2003.

1. Introduction

[2] After more than 25 years of activity, the Voyager 1 spacecraft is the farthest active spacecraft from the Sun. It is now reaching the outer limit of the heliosphere, which is the region of space filled with the expanding solar wind. The heliopause is a contact discontinuity which separates the solar plasma from interstellar plasmas. This region has long been the subject of theoretical speculations but may soon become the object of in situ measurements.

[3] Because of charge exchange coupling between solar protons and neutral hydrogen atoms, we expect that the hydrogen distribution in the outer heliosphere will be affected by the proximity of the heliospheric interface. Early studies of the hydrogen distributions have been focusing on the inner heliosphere. The hot model [*Thomas*, 1978] can be considered as a standard model for the hydrogen distribution within 40 AU of the Sun. However, at the present position of Voyager 1, the standard model assumes a constant density distribution. The work of *Baranov and Malama* [1993] has shown that it is not so. Figure 1 (using distributions from *Izmodenov et al.* [2001]) presents a plausible picture of the outer heliosphere hydrogen distribution. The heliospheric region is marked by the existence of a pile-up of neutral hydrogen following the charge exchange between interstellar neutrals and decelerated interstellar protons. A detailed analysis of this is given by *Izmodenov et al.* [2001].

[4] However, a better understanding of this phenomenon requires the data that Voyager 1 can provide because of its unprecedented position. This paper presents results obtained by the Ultra-Violet Spectrometer, UVS/Voyager 1 [*Broadfoot et al.*, 1977], concerning the interplanetary Lyman α emission. This emission, still very intense at 85 AU from the Sun, is due to the backscattering of solar Lyman α photons by neutral hydrogen atoms in the outer heliosphere. The intensity pattern observed by UVS reflects the distribution of the hydrogen atoms in the outer part of the heliosphere.

[5] The present study will not go into the details of the UVS data processing. These have been described in previous works, mainly *Quémerais et al.* [1995, 2000].

2. Voyager 1 UVS Data

[6] The Voyager Outer Heliosphere scans were first implemented in 1993 to study the interplanetary glow and the hydrogen distribution in the outer heliosphere. From 1993 to 1998 a series of scans were performed by both UVS instruments on board Voyager 1 and Voyager 2. The UVS on board Voyager 2 was shutdown at the end of

0148-0227/03/2003JA009871$09.00

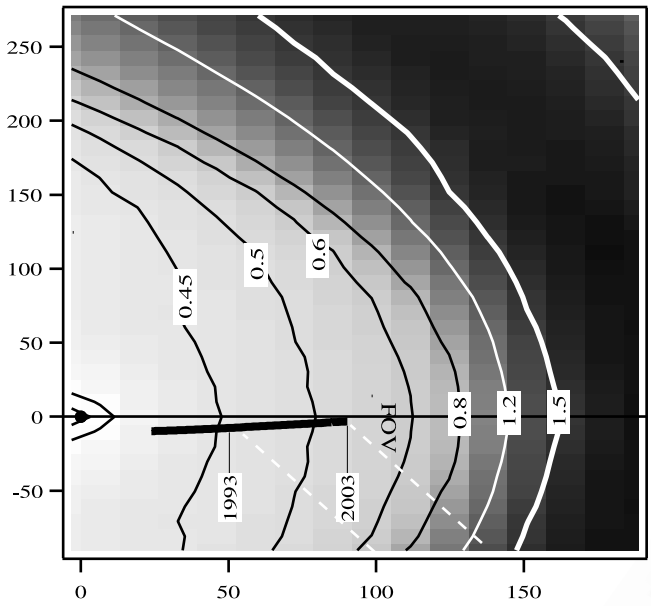

Figure 1. Contour plot of a model of the hydrogen density in the heliosphere. The density values are relative to the assumed value in the interstellar medium. The X and Y axes are in AU from the Sun. The figure also shows the trace of the path of the Voyager 1 spacecraft in the outer heliosphere. The hydrogen wall is shown by the dark color code. Voyager 1 is headed roughly towards the upwind direction (on the right) at a velocity of 3.6 AU per year.

1998 due to power constraints. As of early 2003, the UVS on board Voyager 1 is still performing regular observations although a shutdown of the scanning platform due to power constraints is expected to take place within the year 2003.

[7] Studying the outer heliosphere Lyman α glow over a solar cycle requires an accurate knowledge of the actual variations of the solar illuminating flux during this period. Previous studies have shown that this is not so easy [*Pryor et al.*, 1992; *de Toma et al.*, 1997]. Our original idea was to alleviate this problem by performing scans over a great circle in the sky going through the upwind and downwind directions. The downwind direction is seen close to the Sun because of the position of the spacecraft and downwind observations could be used to follow the solar flux variations and allow for an accurate correction of the upwind observations. This was not implemented because the downwind observations also reflect changes of the solar ionization parameters which determine the hydrogen number density in the inner heliosphere. Although this effect is damped by the distance between the Voyager 1 spacecraft and the Sun, it is large enough to be seen in the data.

[8] The data used here have been described extensively in previous works [*Quémerais et al.*, 1995, 2000]. Information concerning line of sight, data processing, and spacecraft position can be found in these papers. Here we concentrate on two series of scans performed by UVS on Voyager 1 between 1993 and the end of 2002.

[9] Shown in Figure 2 are the two types of outer heliosphere scans performed by UVS/Voyager 1 used here. Both scan types begin near the downwind direction which is close to the direction of the Sun (marked by a cross in the figure) and move to the upwind direction following the trace of a plane. There are about 20 points in each scan, roughly one every 10 degrees. In this figure we have added the trace of the galactic plane (dotted line) with the galactic center within 20 degrees of the upwind direction. The two types of scans, called type A and B afterward, are identical in the downwind hemisphere and are separated by roughly 15 degrees in the upwind direction. Type B was introduced at the end of 1994 because we found that type A was too nearly tangential to the galactic plane. Type B crosses the galactic equator more rapidly and extends to lower galactic latitudes. Type A and Type B are now performed alternately. We have analyzed 37 scans of type A and 39 of type B.

[10] As mentioned by *Quémerais et al.* [1995], a possible contamination of the nine spectral channels used to infer the H Lyman α brightness is possible. Some spectra show a faint "skirt" with a spectral shape similar to a stellar profile. This may be due to some stellar light getting in the field of view or to some stellar emission scattered by dust. This emission is very small and has no component at the Lyman α wavelength because interstellar hydrogen absorbs all interstellar Lyman α photons. However since we integrate over the nine channels centered on the Lyman α wavelength to get the UVS Lyman α data, we must get rid of stellar components around 121.6 nm. To do that we fit the central part (121.6 nm) of an uncontaminated UVS Lyman α spectrum to the spectrum showing a stellar component. The uncontaminated spectrum gives the instrumental response (Point Spread Function) of the narrow backscattered Lyman α line shape and all UV background spectra should have the same shape. The integral of the fitted spectrum is

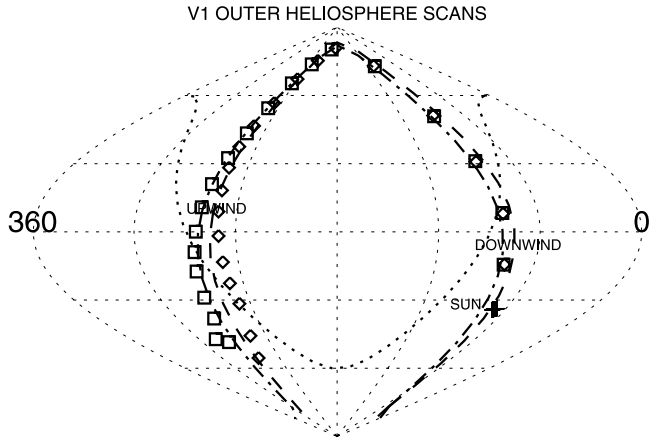

Figure 2. Representation of the two main types of outer heliosphere scans performed by Voyager 1 since 1993. The values are in ecliptic coordinates. The diamonds are for type A scans and the squares for type B. The trace of the galactic plane is shown by the dotted line. The mean plane of each type of scan is shown by the dashed and dash-dot lines (great circle). The points are slightly off the average plane to avoid stars in the Field of View. The positions of the Sun in the sky from 1993 to 1998 are shown by crosses. The numbers 0 and 360 show the ecliptic longitude value.

used as the corrected measurement. This correction has been applied to fewer than three points per map.

2.1. Solar Lyman α Flux Variations

[11] The solar Lyman α flux which is the source of the photons backscattered in the interplanetary medium varies at different time scales. During the 11-year cycle, the flux ratio between minimum and maximum of solar activity is close to 1.8 [*Woods et al.*, 2000]. On the time scale of a day the full disk integrated flux can change by up to 10% during solar maximum. This causes the well-known 27-day modulation of solar data because of the solar rotation period as seen from the Earth. This modulation is clearly visible for instance in the SWAN/SOHO data, a Lyman α photometer studying the interplanetary background in the inner heliosphere [*Bertaux et al.*, 2000].

[12] However, as shown by model calculations made by *Quémerais et al.* [1996a, 1996b], at large distance from the Sun the day to day variations are very much damped by multiple scattering effects. In the outer heliosphere there is almost no contribution to the interplanetary glow from photons coming straight from the Sun. They all have been multiply scattered. As a consequence, the source region on the Sun is not simply the one facing the observer but is spread over the whole Sun. In what follows we will neglect the effect of the 27-day modulation on the solar Lyman α data. To estimate the solar flux for a given observation, we use the database produced by *Woods et al.* [2000] which combines various data sets obtained from the Earth and is regularly updated. When actual solar Lyman α flux measurements are not available they use proxies to fill the gaps. To take into account the damping effect on a daily scale, we perform a gliding mean on the data over a solar period (27 days) centered on the observation date (± 13 days).

[13] It must be noted also that hydrogen atoms in the interplanetary medium can only scatter the Lyman α photons in the core of the solar line. This line is roughly 1 Angström wide which corresponds to a doppler shift from solar rest frame of about ± 150 km/s. In the interplanetary medium the hydrogen atom velocity relative to the Sun is less than 30 km/s, so only a narrow band at the core of the line illuminates the interplanetary hydrogen atoms. The measurements used to estimate the solar flux at a given date correspond to the integrated line. Although there is still a possibility that the ratio of the core intensity to the integrated intensity is not constant with the changes of solar activity [*Lemaire et al.*, 2002], in this paper we will assume that this ratio is constant.

[14] Figure 3 shows the variations of the solar Lyman α integrated flux as seen from the Earth between 1993 and 2003. The thick line shows a gliding average performed over one solar rotation. The diamonds correspond to the times when the outer heliosphere scans were performed (both A and B types). On this plot, the smoothed integrated solar flux varies between 3.5×10^{11} and 6×10^{11} photons cm^{-2} s^{-2} at 1 AU.

2.2. Excess in the Upwind Direction

[15] We have reported in previous works [*Quémerais et al.*, 1995, 2000] that each individual scan presents an excess in the upwind direction. This translates into the fact that the upwind to downwind intensity ratio is higher than the value

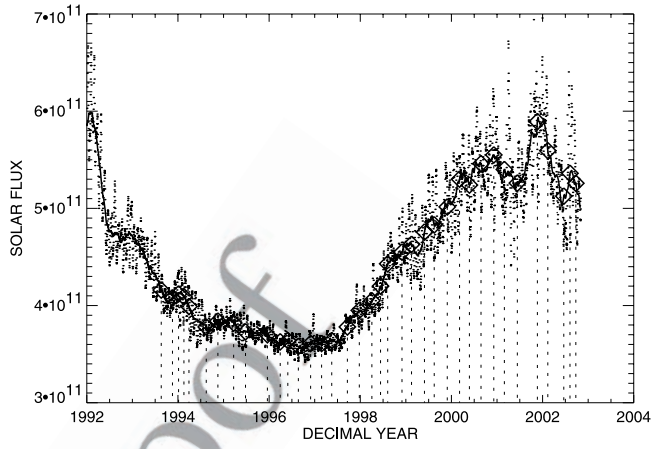

Figure 3. Solar Lyman α line flux data between 1992 and 2003. The thick curve shows a 27-day gliding mean. The data are based on SOLSTICE/UARS measurements. The data gaps are filled by other solar indices. The dates of the UVS/V1 observations are shown by the diamonds. The Y axis is in units of photons cm^{-2} s^{-1} $Å^{-1}$.

derived from modeling. The upwind excess still appears on the latest scans. Unfortunately, because of the combined uncertainty introduced by stellar contamination in some spectra and variability of the downwind hemisphere due to solar cycle variations, it is not possible to clearly identify the origin of this excess.

[16] *Quémerais et al.* [1996a, 1996b] suggested two possible sources for this excess. The first one is an increase of the hydrogen number density as the spacecraft gets closer to the heliospheric interface where a pile-up of neutral hydrogen caused by charge-exchange with protons is expected [*Baranov and Malama*, 1993]. The second possible source is H Lyman α emission from HII regions of the galaxy. Random recombination of electron-proton pairs could lead to some emission of Lyman α photons. The proximity between the upwind direction and the possible location of the H wall and the galactic plane suggests that the observed excess could be a combination of these two effects.

[17] It has been concluded that looking at the excess over a solar cycle would allow us to determine whether the excess shows modulations compatible with the solar flux variations. Emission from a hydrogen pile-up would reflect variations of the solar flux whereas emission from HII regions is expected to remain constant.

[18] We have not yet reached a conclusion because this analysis requires a very good model fitting the downwind data which are affected by the variation of the solar parameters for ionization. Data obtained within the inner heliosphere should be used in conjunction with UVS data to try and follow this variation more accurately.

2.3. Radial Variation of Intensity With Distance

[19] This section presents a study of the radial variation of the upwind intensity as a function of the distance to the Sun. Previous studies of the radial decrease of the upwind data have been presented before [*Hall et al.*, 1993; *Quémerais et al.*, 2000]. As we will show, the conclusion of such a

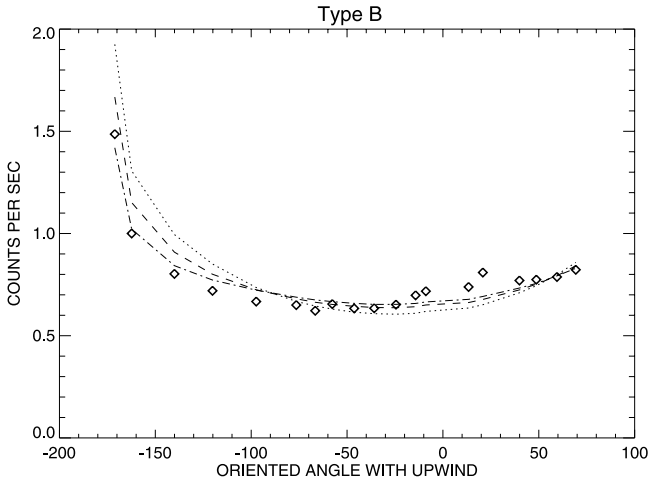

Figure 4. Average of the first four type B maps used as a reference to compute the radial variation of the upwind intensity. UVS data are diamonds. The sunward direction is close to downwind (−180 degrees). The angle is measured from the upwind direction. To compute the coefficient we used only the points in the flat upwind hemisphere (less than 90 degrees from upwind). The three lines show different models with different slopes in hydrogen density number. The dotted line corresponds to a hot model, i.e., with a constant density value. The dashed line is derived from a two-shock model with an electron density of 0.1 cm^{-3} in LISM. The dash-dot line comes from a two-shock model with an electron density of 0.21 cm^{-3} in LISM. They all find a flat intensity distribution in the upwind hemisphere.

study depends very much on the way the data are corrected for solar flux variations. It is also necessary to reduce the effect of residual stellar contamination when applicable.

[20] To decrease the uncertainty due to the contamination of the UVS data by stellar light we have used the following scheme. First, as shown in Figure 4, the intensity distribution pattern in the upwind hemisphere is rather flat for an observer beyond 50 AU. The three models shown in the figure correspond to 3 types of models presented by *Quémerais et al.* [1996a, 1996b]. They assume different values of the electron density in the LISM, thus leading to different slopes for the hydrogen number density in the outer heliosphere. One is a hot model, i.e., the slope is zero. The other two models assume LISM electron number density values of 0.1 and 0.21 cm^{-3}, respectively. The aim of Figure 4 is to show that all models, with or without a strong interface, expect that the Lyman α intensity pattern within 90 degrees of the upwind direction is nearly constant. This is due to the fact that the hydrogen wall is still far away from the observer. The different models differ only by the mean value of the intensity within 90 degrees of upwind and also by the upwind to downwind intensity ratio. By averaging the first maps of each type of scans and excluding all points showing stellar contamination, we have obtained an average map for both types A and B. The example of type B is shown in Figure 4. As models have shown, in the upwind hemisphere, i.e., within 90 degrees from upwind, this shape is expected to remain flat. We have then computed for each scan the mean ratio of the upwind hemisphere data with the upwind hemisphere data of the average scan. This includes only the points which are within 90 degrees of the upwind direction, the flat area in Figure 4. By doing this we expect to decrease the influence of residual stellar contamination because it affects only a few points and not the 10 to 12 points used to determine the ratio.

[21] The results of the ratio as a function of distance to the Sun for both types A and B are shown in Figures 5 and 6, respectively (diamonds linked by a dotted line). Both figures clearly show a variation which is similar to the solar cycle variation of the Lyman α solar flux with a minimum at 65 AU which corresponds to 1996. Note that the small bump appearing in early 2002 in Figure 3 appears at the same date for both types of scans (around 85 AU). The triangle joined by the thick lines show the ratio corrected for solar flux variation using the values derived from Figure 3. For each date of observation we have computed the flux value from the thick line (smoothed curve) of Figure 3. The correction factor applied to the data is equal to the ratio of the flux value for the date of observation with a reference flux value. This reference flux value is chosen to be the one corresponding to the first observation of the type of scans, i.e., the correction factor is equal to 1 for the first point of each type of scan. On both figures, we find that roughly after 1997 (beyond 70 AU), the upwind intensity curve flattens strongly. Obviously, the solar flux correction is not perfect, as shown by two features appearing for both types of scans at the end of 1997 (65–70 AU) and in 1999 (75 AU).

[22] The flattening of the curve after 1997 corresponds to a distance to the Sun of roughly 70 AU. The intensity decrease with radial distance can be represented by a function r^{α} as done by *Hall et al.* [1993]. In that case, before 1998 the UVS/Voyager 1 data show a decrease characterized by $\alpha = -1.58 \pm 0.02$ when corrected for the

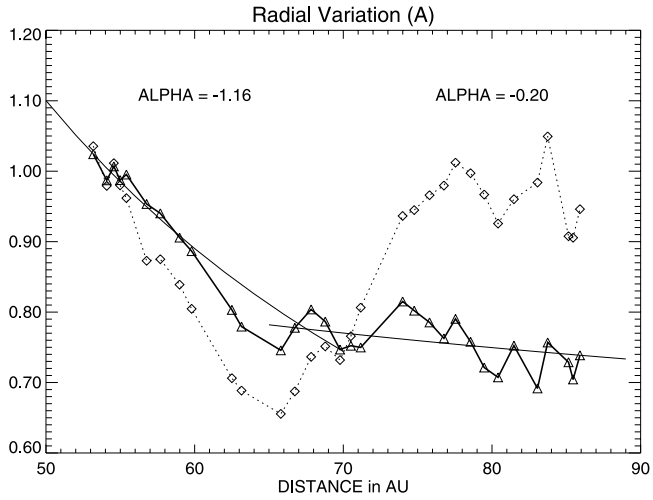

Figure 5. Variation of the upwind intensity data for type A maps as a function of distance to the Sun. The diamonds show the data uncorrected for solar flux variation and the triangles show the data corrected for flux variations. The correction is derived from Figure 3. Estimates for the power law coefficient before and after 1998 (70 AU) are also given. In the text we give the power law coefficient of the combined data A and B.

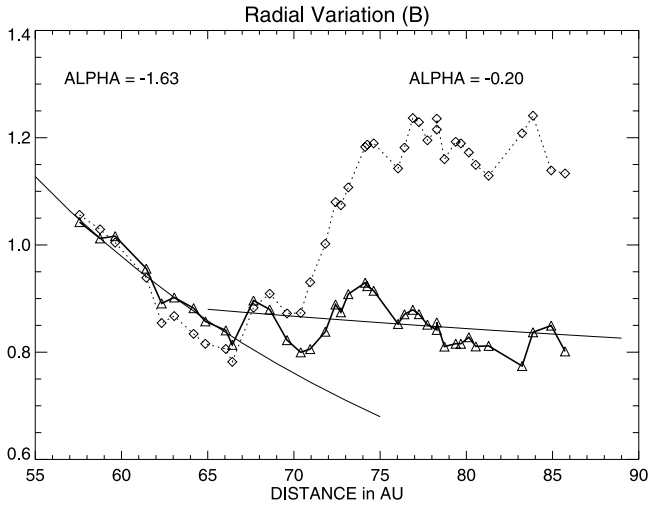

Figure 6. Variation of the upwind intensity data for type B maps as a function of distance to the Sun. The time of observation is also shown at the bottom of the graph. The diamonds show the raw data and the triangles show the data corrected for flux variations. Estimates for the power law coefficient before and after 1998 (70 AU) are also given. In the text we give the power law coefficient of the combined data A and B.

Lyman α flux variations. After 1998 the data show a radial decrease coefficient α equal to -0.22 ± 0.07. These values have been determined by combining both types A and B.

[23] A previous analysis by *Hall et al.* [1993] had found that the radial decrease coefficient between 30 and 35 AU was equal to -0.35 ± 0.05. The value of alpha found here between 50 and 65 AU shows a much steeper gradient than the one reported by these authors. We do not have a clear explanation on the discrepancy, but we suspect that it is partly due to the use of a different database to correct the Lyman α solar flux. In the early 1990s the SME flux estimates were the reference for the absolute calibration. Comparisons with the UARS/Solstice measurements have shown [*Pryor et al.*, 1992; *de Toma et al.*, 1997; *Tobiska et al.*, 1997] that there is a large discrepancy in terms of absolute values but also maximum to minimum ratio. The latest comprehensive data set of solar Lyman α flux produced by *Woods et al.* [2000] has resolved this issue. It would be interesting to re-analyze the data set used by *Hall et al.* [1993] to check the actual value of the decrease coefficient.

[24] Qualitatively, the conclusion presented by *Hall et al.* [1993] is still valid. Indeed, for a constant density in the outer heliosphere (no interface model), the radial decrease coefficient varies between -1 as in the optically thin approximation (inner heliosphere) and an asymptotic value of -2 for a large optical thickness at line center [*Hall et al.*, 1993]. For Voyager 1 using a SOLSTICE based correction, we find a value larger than -1 after 65 AU which is not compatible with the classical hot model which density is nearly constant farther than 50 AU from the Sun [*Quémerais*, 2000].

3. Model Description

[25] The model used in this section has been detailed by *Quémerais and Izmodenov* [2002]. It is based upon computations of hydrogen distributions in the heliosphere including effects of the heliospheric interface [*Baranov and Malama*, 1993; *Izmodenov et al.*, 2001]. Using the density, velocity, and temperature distributions derived from this model as inputs, we compute the radiation field following the scheme developed by *Quémerais* [2000]. This model takes into account multiple scattering and uses the angle dependent partial frequency redistribution function to describe the scattering process. This allows us to compute the interplanetary Lyman α glow line profile anywhere in the heliosphere. Results in the inner heliosphere (intensity and line shape) have been presented by *Quémerais and Izmodenov* [2002]. Here we show model results relevant to the analysis of the UVS/Voyager 1 data between 1993 and 2000. For reference, the parameters of the hydrogen distribution model are given in Table 1.

4. Variation With Solar Distance

[26] In this section we consider the variations of interplanetary background intensity as a function of distance between the observer and the Sun. This study has been made assuming an observer moving away from the Sun in the upwind direction, which is roughly the direction where both Voyager spacecraft are headed. Unfortunately, line shift and line width results will not apply to these data because the spectral resolution of the UVS instruments does not allow for a spectral analysis of the Voyager outer heliosphere UV data.

4.1. Intensities and Gradients

[27] The radial dependence of the upwind intensity is shown in Figure 7. The full radiative transfer result is shown by the solid line and the usual approximations are shown for comparison. It is clear here that no approximation can be applied outside a few AU from the Sun.

[28] Figure 8 is derived from the results of Figure 7. It shows a quantity introduced by *Hall et al.* [1993] and that we will call the radial coefficient and note α. This coefficient measures the slope of the quantity considered. If f is the observed quantity, the radial coefficient α_f is defined by

$$\alpha_f = \frac{r}{f}\left(\frac{\partial f}{\partial r}\right) \tag{1}$$

[29] Here, r is the distance to the Sun. This means that locally $f(r)$ is proportional to r^{α_f}. If α_f is constant then the observed quantity is simply described by a power law of the solar distance.

Table 1. Parameters of the Hydrogen Distribution Model

LIC Parameters	
Proton number density	0.04 cm^{-3}
Hydrogen number density	0.2 cm^{-3}
Bulk velocity	25 km/s
Temperature	5700 K
Solar Parameters	
Radiation pressure to gravitation (μ)	0.75
Proton number density at Earth	7 cm^{-3}
Solar wind velocity	450 km/s

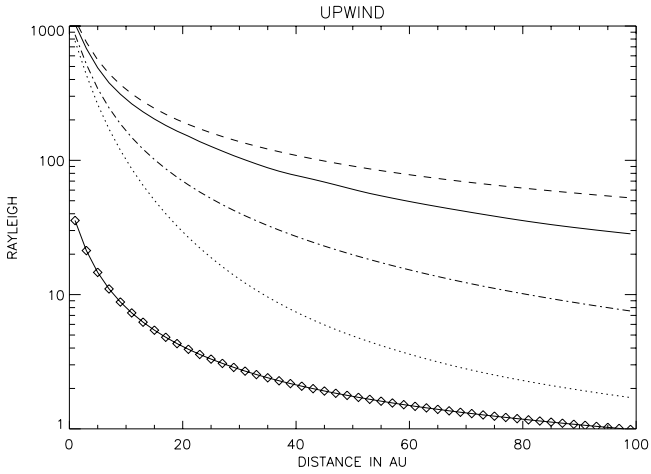

Figure 7. Model upwind intensity as a function of solar distance of the observer. The full radiative transfer calculation (three populations given by *Quémerais and Izmodenov* [2002]) is shown by the solid line. The optically thin calculation is shown by the dashed line. We have added the self-absorbed result (dash-dot) and the primary term (direct due to solar excitation, dotted line) [see *Quémerais and Izmodenov*, 2002]. The diamonds show the intensity due to the hot population of neutral hydrogen atoms due to charge exchange between ISM neutrals and solar protons in the heliosheath.

[30] *Hall et al.* [1993] have noticed that for a hot model, the density is constant in the outer heliosphere, i.e., its radial coefficient is equal to zero. In that case the optically thin intensity has a radial coefficient equal to -1 and the radiative transfer intensity converges asymptotically towards -2. They suggested also that a positive gradient of density caused by a hydrogen wall will shift all those gradients toward less negative values.

[31] *Quémerais* [2000] found the following numerical values for the hot model between 80 and 100 AU. The density radial coefficient is zero, the optically thin coefficient is -0.99 and the full radiative transfer coefficient is -1.46.

[32] In Figure 8 we show the values of α corresponding to the interface model. Between 80 and 100 AU, the three-population density [*Quémerais and Izmodenov*, 2002] has a radial coefficient equal to 0.24 (not shown in figure), the optically thin intensity gives -0.79, and the multiple scattering intensity gives -1.06. It is interesting to note that the radial decrease of the upwind intensity is very close to the decrease found for a hot model in the optically thin approximation (For a constant density and optically thin approximation the emissivity is proportional to $1/r^2$ and the intensity, its integral over the line of sight, is proportional to $1/r$). Note also that the modulation seen around 40 AU in the radial coefficient of the multiple scattering result is caused by the Monte Carlo algorithm. In the same figure (Figure 8) we have also added the radial coefficient found by *Quémerais* [2000] for a hot model matching the three-population results at one AU in the upwind direction. It is interesting to note that in the region within 30 AU from the Sun the radial coefficients of both models are identical. This means that a spacecraft must be at least farther than 40 AU from the Sun before this type of study can be used to discriminate between hot model distributions and interface induced hydrogen distributions if only intensity measurements are considered. Line shape diagnostics can be performed at the orbit of the Earth [*Clarke et al.*, 1995].

4.2. Data to Model Ratios

[33] In Figure 9 we show the ratio of the data of Figures 5 and 6 divided by model computations. Both types of scans have been put together on the plots showing that the results are not dependent on the actual line of sight. The ratio is plotted as a function of the distance between Voyager and the Sun. There are four panels in the figure. The top left panel corresponds to the hot model combined with radiative transfer modeling using the Angle Dependent Partial Frequency Redistribution [*Quémerais*, 2000]. The top right and bottom left panels are based on hydrogen distributions by *Malama and Baranov* [1993] combined with radiative transfer modeling using Complete Frequency Redistribution [*Quémerais et al.*, 1996a, 1996b]. The two models differ by the value assumed for the electron density in the LISM, 0.1 cm^{-3} and 0.21 cm^{-3}, respectively. The bottom right panel shows the result obtained with the model described by *Quémerais and Izmodenov* [2002].

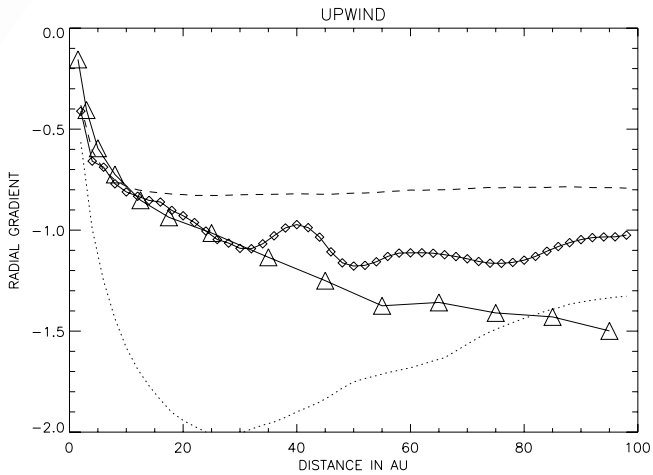

Figure 8. Intensity radial power law coefficient α (called Radial Gradient in the ordinate caption) as a function of solar distance in upwind direction. The Hot Model result is shown by the triangles. This curve has an asymptotic limit of -2. The diamonds show the radial coefficient for the full radiative transfer computation and a density model with interface. (Note that the fluctuation around 40 AU is due to the Monte Carlo method. It reflects a fluctuation present in the density model). At 100 AU it is close to -1. The dashed line shows the three-population optically thin result and the dotted line shows the radial coefficient of the primary term. The positive gradient of the three-population density model modifies the results of the intensity radial coefficient. In the case of the three-population model, the intensity radial decrease is slower than in the case of the hot model. Note that within 30 AU from the Sun, both Hot and three-population models give the same result for the radial coefficient.

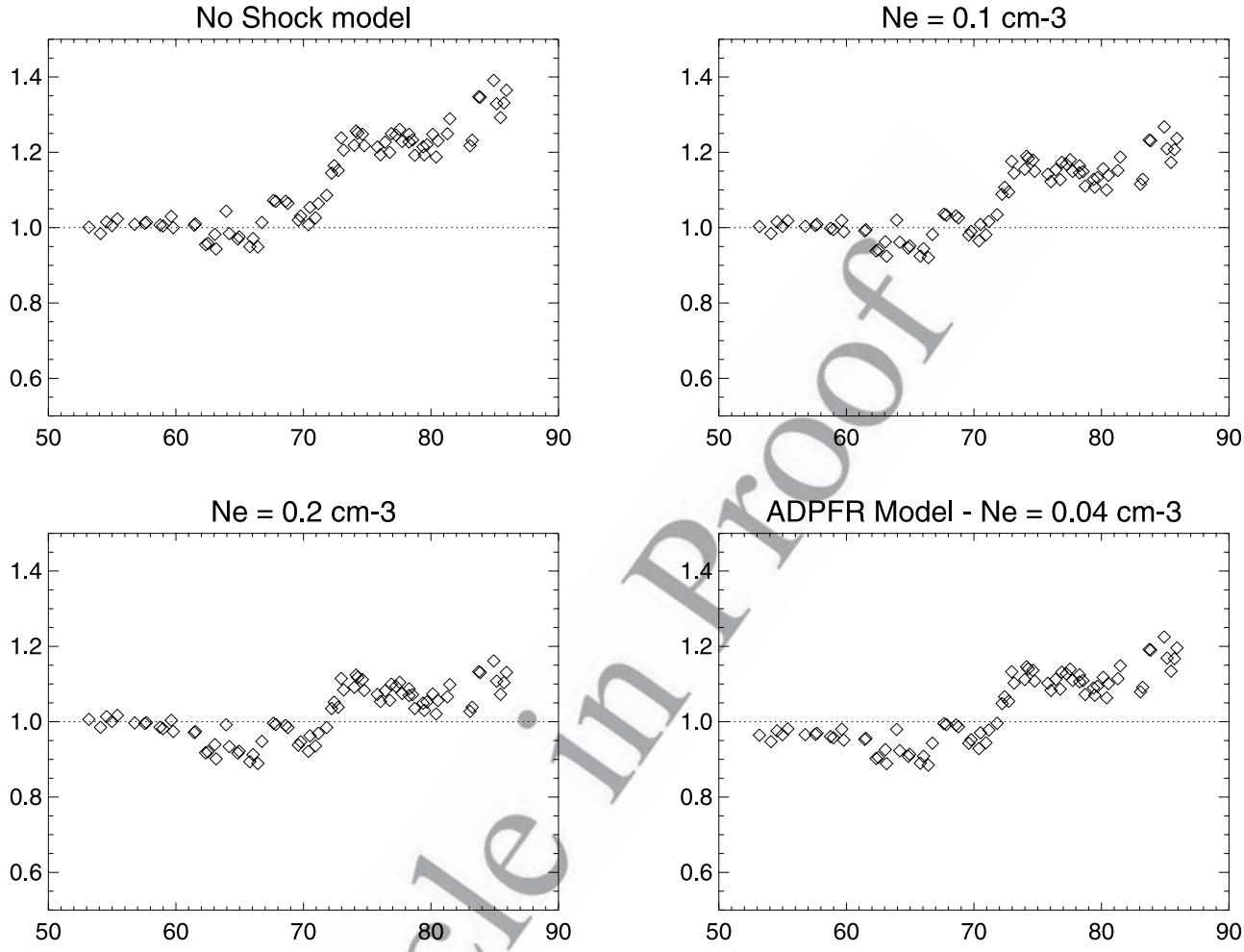

Figure 9. Ratio of solar flux corrected data with four different models of the interplanetary background. For each figure the abscisse is the spacecraft distance to the Sun in AU. The points show the combined results of type A and type B maps. Four different models have been used here. The main difference lies in the hydrogen density distribution assumed for the calculation of the intensity in the outer heliosphere. In the top left panel the hydrogen density is described by a hot model without heliospheric interface. The H number density is constant beyond 50 AU from the Sun. The three other models have been produced by the Baranov group with different electron number density in the LISM which translates into different positions of the H wall. All curves show a steep increase after 70 AU.

[34] The different models have different hydrogen distributions in the outer heliosphere influenced by the position of the interface and the hydrogen wall. Of course for the hot model, the slope coefficient of the density is zero (the hydrogen wall is at infinity).

[35] The curves all show the same features, a rather good agreement before 70 AU and a sharp increase after 70 AU. This shows that the current models do not explain the abrupt flattening of the data observed after 70 AU which translates into a steep increase when we divide the data by a mode. In fact, our models expect a much smoother variation. In the next section we will discuss possible explanations.

5. Conclusion

[36] The data we have presented here have been obtained by UVS on Voyager 1 between 1993 and the end of 2002. They consist of two series of identical scans of 20 points aligned along great circles in the sky going through the downwind and upwind directions. The average separation between two points is 10 degrees. Possible variations of the UVS sensitivity have been checked by comparison of spectral observations of some stars made regularly. We have not found any substantial variation after 1993. We have then concluded that the UVS calibration factor at Lyman α was constant over the whole period of these observations.

[37] First, the general conclusions which have been drawn from the data from 1993 to 2000 are maintained entirely: We find that the ratio between the upwind and downwind intensity measured by the spacecraft, which has the great advantage of being independent of the solar flux, is higher than expected from hot model calculations. This feature, first reported by *Quemerais et al.* [1995], is still seen in the latest maps. Unfortunately, solar cycle variations of the gas distribution close to the Sun, i.e., seen downwind

from the vantage point of Voyager, prevent a definitive analysis of the upwind trend when using the comparison with the downwind signal. However, the observed upwind to downwind data ratio is always higher than the predicted value from hot model calculations for any set of solar parameters used.

[38] In this work we have concentrated on the study of the radial variation of the upwind hemisphere intensity. These data need to be corrected for solar Lyman α flux variations due to the 11-year solar cycle. To do that we have used the dataset compiled by *Woods et al.* [2000], which is updated on a regular basis.

[39] The solar flux corrected data clearly show two phases:

[40] 1. Before 1998 or 70 AU from the Sun, the data fall off with a power law coefficient α close to -1.5. This value is in good agreement with radiative transfer calculations and a hydrogen number density almost flat or slowly increasing, i.e., far from the hydrogen wall.

[41] 2. After 1998 or 70 AU from the Sun, the upwind intensity curve flattens strongly. The power law coefficient changes to -0.2, which suggests that the hydrogen number density is increasing steeply. Such an increase is faster than what could be expected from a constant source outside the heliosphere.

[42] In the case of our stationary models, those two phases are not compatible because the variations of the upwind intensity is expected to be rather smooth. The intensity is integrated over the line of sight, which is a few tens of AU long. This means that abrupt jumps in density are detected ahead and none of the density models used here could explain this strong flattening after 70 AU. This applies also to a constant source of Lyman α photons outside the heliosphere, like a galactic emission, which can not explain such a fast change in radial variation.

[43] The observed behavior is more likely the result of a phenomenon absent from the present modeling. Possible explanations are of two classes: unexpected (or incorrectly modeled) solar emission, or unsatisfyingly modeled density distribution. We list them here in arbitrary order:

[44] 1. The absence of proportionality between the solar flux as seen from the Earth and the global illumination of the gas in the outer heliosphere. This could be due to the aspherical distribution of the active regions, which are responsible for a large fraction of the Lyman α emission. The outer gas receives a photon flux proportional to the full solar output, while the in-ecliptic observer close to the Sun is more influenced by low latitudes. This should be a minor effect but has to be quantified. Note that Figure 9 shows that there are still some artifacts left over after the solar flux correction. This flux correction needs to be studied on other data of the interplanetary Lyman α background like the measurements of SWAN/SOHO [*Bertaux et al.*, 2000] of the data or the UVS on Galileo [*Pryor et al.*, 2001].

[45] 2. The absence of proportionality between the Lyman α line-integrated solar flux and the flux at line center. This is unlikely, according to recent SUMER measurements [*Lemaire et al.*, 2002].

[46] 3. Finally, we should also consider nonstationary models of the hydrogen distribution in the outer heliosphere. The existence of rather strong cyclical fluctuations of the outer heliosphere neutral hydrogen density in response to cyclical changes of the plasma structure (the so-called ''breathing'' of the heliosphere) have been shown by recent computations by *Izmodenov and Malama* [2002]. They show that an unstable heliospheric interface can modulate the hydrogen number density in the outer heliosphere. In that case, modulation of the H number density may be the cause of this apparent flattening of the radial curve of the upwind data.

[47] 4. More speculatively, a change in the global shape of the heliosphere during the last years, with an increase and inward motion of the hydrogen wall due to changes in external conditions or resulting from the intrinsically unstable character of the interface. In this case this sudden change in the trend could be connected with the absence of detection of 2–3 Khz radio emissions during the present maximum of activity, after two consecutive cycles of presence of these waves. The heliosphere may have returned to a more stable and closed configuration.

[48] **Acknowledgments.** This work was supported in part by INTAS grant 2001-0270 and International Space Science Institute (ISSI) in Bern under ''Physics of the heliotail'' team-project. V.I. was also supported by Russian Foundation for Basic Research (RFBR) grants 01-02-17551, 03-02-06124, and 01-01-00759. Work at The University of Arizona was supported under NASA grant NAG5-7089.

[49] Shadia Rifai Habbal thanks Wayne Robert Pryor and Howard S. Ogawa for their assistance in evaluating this paper.

References

Baranov, V. B., and Y. G. Malama, Model of the solar wind interaction with the local interstellar medium—Numerical solution of self-consistent problem, *J. Geophys. Res.*, *98*, 15,157, 1993.

Broadfoot, A. L., et al., Ultraviolet spectrometer experiment for the Voyager mission, *Space Sci. Rev.*, *21*, 183, 1977.

Bertaux, J. L., E. Quémerais, R. Lallement, E. Lamassoure, W. Schmidt, and E. Kyrölä, Monitoring solar activity on the far side of the Sun from sky reflected Lyman alpha radiation, *Geophys. Res. Lett.*, *27*, 1331, 2000.

Clarke, J. T., R. Lallement, J.-L. Bertaux, and E. Quemerais, HST/GHRS Observations of the interplanetary medium downwind and in the inner solar system, *Astrophys. J.*, *448*, 893, 1995.

de Toma, G., E. Quemerais, and B. R. Sandel, Long-term variation of the interplanetary H Ly alpha glow: Voyager measurements and implications for the solar H Ly alpha irradiance, *Astrophys. J.*, *491*, 980, 1997.

Hall, D. T., D. E. Shemansky, D. L. Judge, P. Gangopadhyay, and M. A. Gruntman, Heliospheric hydrogen beyond 15 AU—Evidence for a termination shock, *J. Geophys. Res.*, *98*, 15,185, 1993.

Izmodenov, V., M. Gruntman, and Y. G. Malama, Interstellar hydrogen atom distribution function in the outer heliosphere, *J. Geophys. Res.*, *106*, 10,681, 2001.

Lemaire, P., C. Emerich, J.-C. Vial, W. Curdt, U. Schühle, and K. Wilhelm, Variation of the full Sun hydrogen Lyman α and β profiles with the activity cycle, in *Proceedings of the SOHO 11 Symposium on From Solar Min to Max: Half a Solar Cycle with SOHO, 11–15 March 2002, Davos, Switzerland, ESA SP-508*, edited by A. Wilson, pp. 219–222, ESA Publ. Div., Noordwijk, Netherlands, 2002.

Pryor, W. R., J. M. Ajello, C. A. Barth, C. W. Hord, A. I. F. Stewart, K. E. Simmons, W. E. McClintock, B. R. Sandel, and D. E. Shemansky, The Galileo and Pioneer Venus ultraviolet spectrometer experiments—Solar Lyman α latitude variation at solar maximum from interplanetary Lyman α observations, *Astrophys. J.*, *394*, 363, 1992.

Pryor, W. R., A. I. F. Stewart, K. E. Simmons, J. T. Clarke, J. M. Ajello, W. K. Tobiska, and G. R. Gladstone, Remote sensing of H from Ulysses and Galileo, *Space Sci. Rev.*, *97*, 393, 2001.

Quémerais, E., Angle dependent partial frequency redistribution in the interplanetary medium at Lyman alpha, *Astron. Astrophys.*, *358*, 353, 2000.

Quémerais, E., and V. Izmodenov, Effects of the heliospheric interface on the interplanetary Lyman alpha glow seen at 1 AU from the Sun, *Astron. Astrophys.*, *396*, 269, 2002.

Quémerais, E., B. R. Sandel, R. Lallement, and J. L. Bertaux, A new source of Lyα emission detected by Voyager UVS: Heliospheric or galactic origin?, *Astron. Astrophys.*, *299*, 249, 1995.

Quémerais, E., B. R. Sandel, and G. de Toma, 26-day modulation of the sky background LY alpha brightness: Estimating the interplanetary hydrogen density, *Astrophys. J.*, *463*, 349, 1996a.

Quémerais, E., Y. G. Malama, B. R. Sandel, R. Lallement, J. L. Bertaux, and V. B. Baranov, Outer heliosphere Lyman α background derived from two-shock model hydrogen distributions: Application to the Voyager UVS data, *Astron. Astrophys.*, *308*, 279, 1996b.

Quémerais, E., B. R. Sandel, J. L. Bertaux, and R. Lallement, Outer Heliosphere Ly-a Measurements: 1993 to 1998, *Astrophys. Space Sci.*, *274*, 123, 2000.

Thomas, G. E., The interstellar wind and its influence on the interplanetary environment, *Annu. Rev. Earth Planet. Sci.*, *6*, 173, 1978.

Tobiska, W. K., W. R. Pryor, and J. M. Ajello, Solar hydrogen Lyman-alpha variation during solar cycles 21 and 22, *Geophys. Res. Let.*, *24*, 1123, 1997.

Woods, T., W. K. Tobiska, G. J. Rottman, and J. R. Worden, Improved solar Lyman alpha irradiance modeling from 1947 through 1999 based on UARS observations, *J. Geophys. Res.*, *105*, 195, 2000.

E. Quémerais, J.-L. Bertaux, and R. Lallement, Service d'Aéronomie du CNRS, BP 3, 91371, Verrières le Buisson, France. (Eric.Quemerais@aerov.jussieu.fr; jean-loup.bertaux@aerov.jussieu.fr; rosine.lallement@aerov.jussieu.fr)

B. R. Sandel, Lunar and Planetary Laboratory, 1040 East Fourth Street, Room 901, University of Arizona, Tucson, AZ 85721, USA. (sandel@arizona.edu)

V. Izmodenov, Institute for Problems in Mechanics, Moscow State University Vorob'evy Gory, Main Building MSU, Moscow 119899, Russia. (izmod@ipmnet.ru)